Journal of
Micro/Nanolithography, MEMS, and MOEMS

SPIEDigitalLibrary.org/jm3

Light confinement effect of nonspherical nanoscale solid immersion lenses

Myun-Sik Kim
Toralf Scharf
David Nguyen
Ethan Keeler
Skyler Rydberg
Wataru Nakagawa
Gaël Osowiecki
Reinhard Voelkel
Hans Peter Herzig

SPIE

Light confinement effect of nonspherical nanoscale solid immersion lenses

Myun-Sik Kim
Ecole Polytechnique Fédérale de Lausanne
Optics & Photonics Technology Laboratory
Neuchâtel CH-2000, Switzerland
and
SUSS MicroOptics SA
Rouges-Terres 61
Hauterive CH 2068, Switzerland
E-mail: kim@suss.ch

Toralf Scharf
David Nguyen
Ecole Polytechnique Fédérale de Lausanne
Optics & Photonics Technology Laboratory
Neuchâtel CH-2000, Switzerland

Ethan Keeler
Skyler Rydberg
Wataru Nakagawa
Montana State University
Department of Electrical and Computer Engineering
Bozeman, Montana 59717-3780

Gaël Osowiecki
Ecole Polytechnique Fédérale de Lausanne
Optics & Photonics Technology Laboratory
Neuchâtel CH-2000, Switzerland

Reinhard Voelkel
SUSS MicroOptics SA
Rouges-Terres 61
Hauterive CH 2068, Switzerland

Hans Peter Herzig
Ecole Polytechnique Fédérale de Lausanne
Optics & Photonics Technology Laboratory
Neuchâtel CH-2000, Switzerland

Abstract. We report on the light confinement effect observed in nonideally shaped (i.e., nonspherical) nanoscale solid immersion lenses (SIL). To investigate this effect, nanostructures of various shapes are fabricated by electron-beam lithography. When completely melted in reflow, these noncircular pillars become spherical, while incomplete melting results in nonspherically shaped SILs. Optical characterization shows that nonideal SILs exhibit a spot size reduction comparable with that of spherical SILs. When the size of the SIL is of wavelength scale or smaller, aberrations are negligible due to the short optical path length. This insensitivity to minor variations in the shape implies a large tolerance in nano-SIL fabrication. [DOI: 10.1117/1.JMM.12.2.023015]

Subject terms: solid immersion lens; nano-fabrication; electron beam lithography; thermal reflow; soft lithography; high-resolution interference microscope.

Paper 13027SSP received Mar. 17, 2013; revised manuscript received May 1, 2013; accepted for publication May 7, 2013; published online Jun. 12, 2013.

1 Introduction

The immersion technique, which improves the imaging performance of a microscope, was first proposed by Hooke in his book *Microscopium* in 1678.[1] Sir Brewster later proposed the immersion of the objective lens in 1812.[2] Similarly, the concept of homogeneous immersion and the immersion objective preceded Ernst Abbe's pioneering work, in which he demonstrated the first oil-immersion lens in developing the imaging theory of microscopy.[3] Abbe also developed the standard measure of performance of an objective lens, the numerical aperture (NA), which is defined as[4]

$$\mathrm{NA} = n \cdot \sin\theta, \tag{1}$$

where θ is the half angle of the focus cone and n is the refractive index of the medium through which the light passes [see Fig. 1(a)]. The immersion technique is directly based on Eq. (1) as a factor n larger NA for the same focusing angle.

Until Mansfield et al. developed a new immersion concept in 1990, termed the solid immersion lens (SIL),[5] the main stream of research had focused on improving the performance of the objectives with liquid immersion and by finding better immersion liquids. The concept of solid immersion is derived from the idea that focusing in the center of a hemispherical solid leads to normal incidence of the rays with respect to the spherical interface, which is depicted in Fig. 1(d). In this way, one can avoid the refraction at the interface between the spherical solid and the surrounding medium (e.g., air). It leads to an increment of the NA by a factor of n, the refractive index of the hemispherical

0091-3286/2013/$25.00 © 2013 SPIE

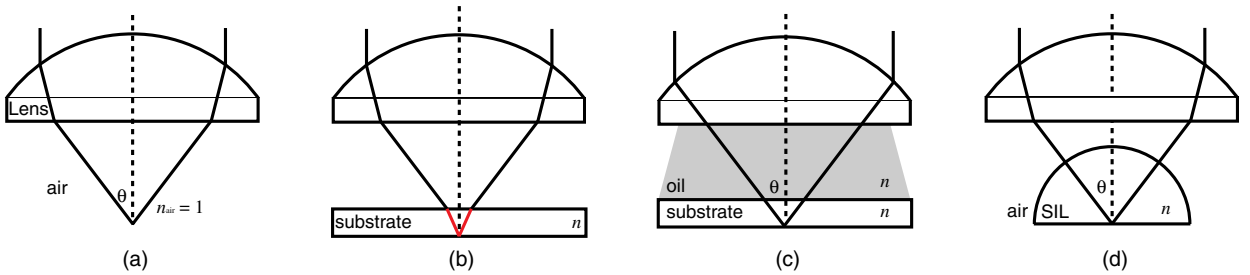

Fig. 1 Working principle of the immersion schemes: (a) focusing in air, (b) focusing through a substrate with a planar interface, where aberrations degrade the optical performance, (c) liquid immersion in oil, and (d) solid immersion using a hemispherical solid medium. The numerical aperture (NA) is a product of the refractive index (n) and the sine of the half-focusing angle (sin θ) [see Eq. (1)].

solid medium [see Eq. (1)]. During the last two decades, numerous studies on SILs and their applications have been carried out. A majority of such studies focused on the macroscopic-size (i.e., millimeter scale) SILs due to the lack of fabrication technologies. Recent advances in micro- and nano-fabrication technologies enabled the development of different types of SILs, including diffractive SILs,[6] micrometer-size SILs,[7–10] nanoscale spherical lenses,[11] and wavelength-scale SILs.[12] In general, for structures smaller than the optical wavelength, design methods for larger devices, such as ray optics, are not applicable. More specifically, subwavelength-scale lenses cannot simply be considered refractive optical surfaces. However, recent experimental work has shown that subwavelength-scale SILs are still expected to produce a reduced-size focal spot,[12] the so-called immersion effect. Recently, we reported the first experimental demonstration of the immersion effect in subwavelength-scale SILs.[13] In fabrication, the ideal case leads to hemispherically shaped SILs. In reality, it is difficult to achieve the exact shape of the ideal design. In this study, we systematically investigate the light confinement effect of nonideally shaped SILs by using different shapes of nano-pillars. When an over-reflow occurs, the noncircular structures, such as square and triangular pillars, are easily transformed into spherical caps. However, in this case, the drawback is an enlarged size in the transverse directions. Thus, we look for the optimal reflow conditions to achieve a minimal expansion of the original size of the nano-pillars. The optical characterization of such small SILs has been realized by using a high-resolution interference microscope (HRIM). The HRIM facilitates complex alignment tasks by the *in situ* monitoring of the illumination beam. The aim of this paper is to report on the optimal reflow conditions for such small nano-pillars and the light confinement effect of nonspherical nano-SILs.

2 Fabrication Processes

The fabrication process consists of three main steps, which are depicted in Fig. 2. First, electron-beam lithography (EBL), which is shown in Fig. 2(a)–2(c), has been used for nano-pattering and structuring. The EBL resist, polymethyl methacrylate (PMMA), has, in general, been considered as a liftoff layer or an etch mask for further fabrication steps rather than a host material for direct nano-structuring. In fact, the PMMA resist is a thermoplastic, and therefore, thermal reflow structuring[14,15] can be applied. This thermal reflow is the second main fabrication step shown in Fig. 2(d). The EBL process is optimized to work with a

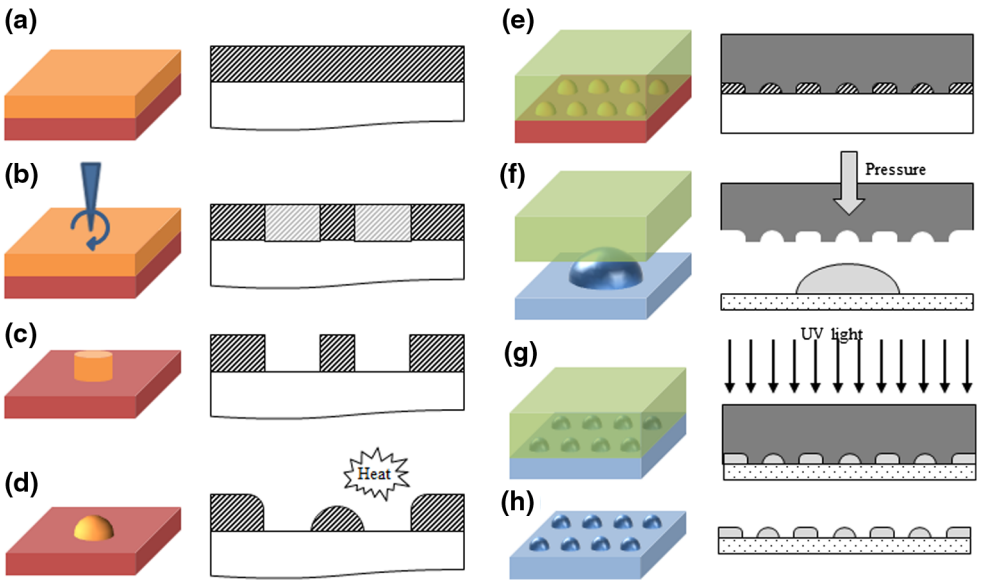

Fig. 2 Schematics of fabrication processes: (a) PMMA resist coting, (b) e-beam lithography exposure, (c) development, (d) thermal reflow, and (e)–(h) soft lithography.

silicon (Si) substrate to enhance the resolution by avoiding electric charging phenomenon caused by nonconductive substrates. For optical characterization in transmission, such nano-structures fabricated on a Si substrate should be replicated on a substrate that is transparent in the visible spectrum. Thus, the final step is the replication process by using soft lithography.[16] In this section, we discuss the detailed fabrication processes of nano-SILs.

2.1 *Electron-Beam Lithography*

The polymer nano-pillars are fabricated using EBL on Si substrates with a thin PMMA resist layer (MicroChem Corp., 950k molecular weight). The Si substrates are used to improve sample conductivity and thereby reduce charging effects. Various sizes of PMMA nano-pillars are fabricated: heights of 200, 250, and 300 nm and widths or diameters of 400 to 600 nm. Example results of the fabricated pillars are shown in the scanning electron microscope (SEM) images of Fig. 3. An area of approximately 4 μm square has been exposed to pattern a pillar in the center. Since PMMA is a positive resist, during the development process the exposed area is removed, leaving a free-standing pillar of PMMA.

2.2 *Thermal Reflow*

A reference temperature for thermal reflow is the glass transition temperature (T_g) of polymers, which is between approximately 110°C and 120°C for PMMA.[17] Note that the T_g of PMMA varies depending on the molecular weight M_w, which also varies depending on the exposure dose of the electron beam.[17] Several studies report that reflow below 120°C led only to smoothing, the reduction of surface roughness, partial reflow, or partial deformation of the structures.[17–19] Therefore, we start with 120°C. The reflow time is as well a governing parameter for proper reflow.

Above 130°C, over-reflow starts to significantly influence the size of the nanostructures not only in the transverse directions but also in the vertical direction (i.e., height). For example, reflow at 140°C for 20 min led to a diameter expansion of approximately 100 nm and a height reduction of approximately 100 nm. A higher temperature, e.g., over 130°C, in general leads to a very rapid reflow and melting process. Therefore, a lower temperature is preferred for slow reflow. Among various conditions, we obtained minimal size variation in width and height when the nano-pillars are reflowed at 120°C for 30 min on a hot plate. The results are shown in the SEM images of Fig. 4.

2.3 *Replication on a Transparent Substrate*

Silicon is opaque in the visible spectrum, which is the designed operating wavelength range of this study. Therefore, the reflowed structures must be replicated on transparent substrates for optical characterization in transmission. To do so, we employ soft lithography, which is a well-established and proven method for the replication of nano-scale structures.[16] A UV-curable polymer (Norland,

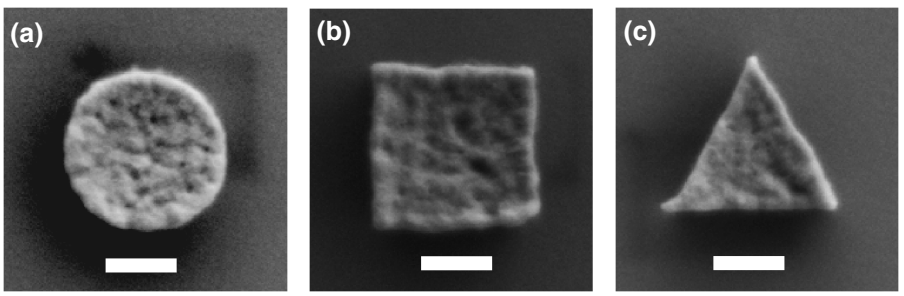

Fig. 3 SEM images of PMMA nano-pillars fabricated on silicon substrates: (a) a cylinder of diameter = 450 nm and height = 250 nm, (b) a square pillar of width = 500 nm and height = 300 nm, and (c) an equilateral-triangular pillar of side length = 520 nm and height = 250 nm. The scale bars indicate 200 nm.

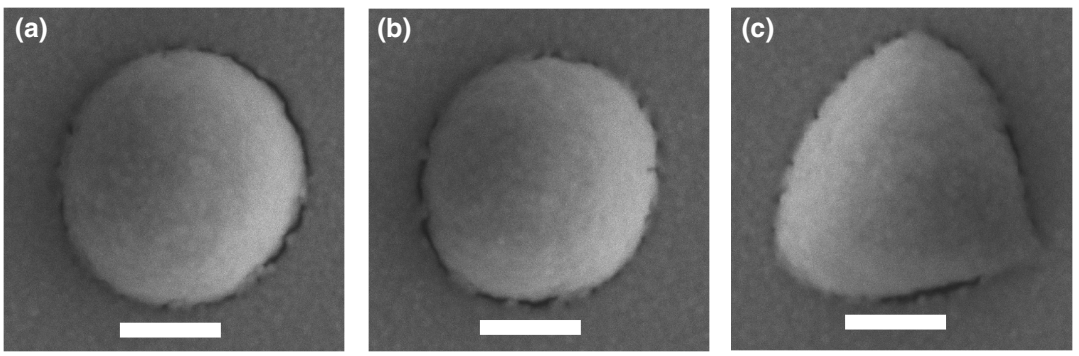

Fig. 4 SEM images of polymer nano-pillars after reflow: (a) a cylinder of diameter = 450 nm and height = 200 nm, (b) a square pillar of width = 400 nm and height = 200 nm, and (c) an equilateral-triangular pillar of side length = 600 nm and height = 200 nm. The scale bars indicate 200 nm.

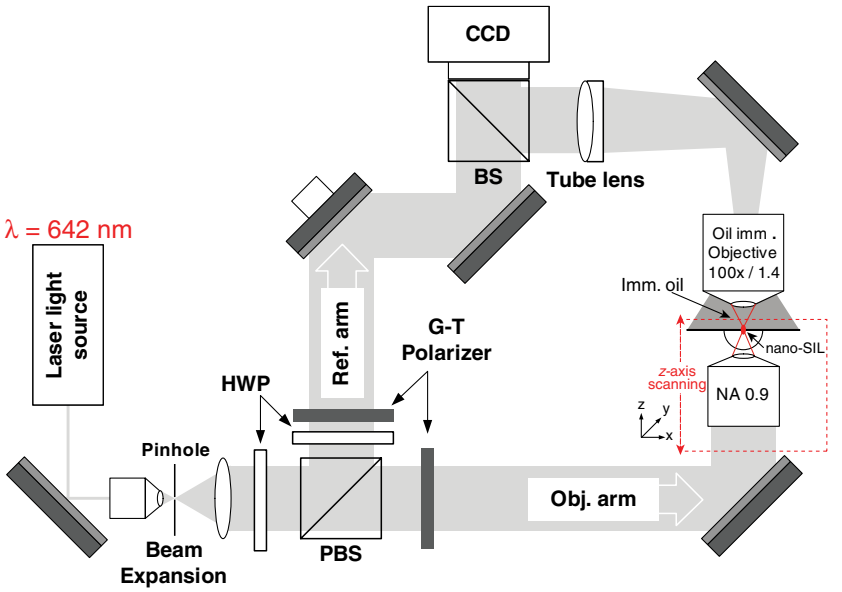

Fig. 5 Schematic of the measurement setup, a high-resolution interference microscope, with the nano-SIL and an NA = 0.9 focusing lens inserted on the sample stage (*z*-axis piezo actuator). A plane wave emerges to the focusing lens at normal incidence. Scanning the nano-SIL together with the focusing lens allows the 3-D intensity measurements.

NOA 65, $n = 1.52$) is used to fill the replication mold, which is made of PDMS (see the schematic of fabrication processes in Fig. 2). The final spherical structures are formed on borosilicate glass cover slips (thickness = 150 μm, $n = 1.52$) by using this PDMS mold.

3 Optical Characterization

3.1 *Measurement Setup*

For optical characterization, we employ a high-resolution interference microscope, which is a proven tool to characterize micro- and nano-optical elements.[20,21] The HRIM operates in transmission with in-line geometry by employing a Mach–Zehnder interferometer as shown in Fig. 5. Note that, in this study, the interferometric function is not utilized. However, the HRIM facilitates the active alignment and the measurements of the three-dimensional (3-D) intensity distributions of highly focused beams. A single mode polarized laser diode (CrystaLaser, 642 nm: DL640-050-3) is employed as a light source, which is expanded and collimated by a spatial filter. This illumination plane wave, which is normally incident upon the illumination element, in our case, the NA = 0.9 focusing objective, propagates along the positive z-axis and is polarized in the x-direction. In the classical interferometric arrangement, a polarizing beam splitter divides intensities among a reference and an object arm with adjustable energy ratio. Half wave plates and Glan–Taylor (G–T) polarizers are used to adjust the intensities and to optimize the contrast of the interference fringes. The sample and the illumination element are mounted on a precision piezo stage with a z-scan range of 500 μm and a nominal accuracy of 1 nm (Mad City Labs, NANO Z500). This z-axis piezo stage is used to precisely define the plane of interest at the highest resolution and measure 3-D light fields through the nano-SIL by scanning the SIL and the focusing lens along the axial direction, as shown in Fig. 5.

3.2 *Verification of Tighter Light Confinement Effect by Nonspherical Nano-SILs*

The fundamental function of the SIL is to reduce the focal spot due to the immersion effect, which improves the resolution in microscopy and lithography applications. Here, we verify the spot-size reduction by applying a highly focused, linearly-polarized beam to the nano-SIL. We compare the spot size created by a spherical-shape SIL [see Fig. 4(a)] with that of the nonspherical-shape SILs [see Fig. 4(b) and 4(c)]. The incident plane wave is focused by an NA = 0.9 objective lens, which is the illumination lens shown in Fig. 5. In the SIL, when this illumination focal spot is off [see Fig. 6], it represents the nonimmersion case; and we set it as a reference for the spot size reduction and the peak intensity enhancement. When this reference focal spot is moved onto the fabricated nano-SILs, the tighter light confinement effect leads to a smaller focal spot and an enhancement of the peak intensity. The nonimmersion

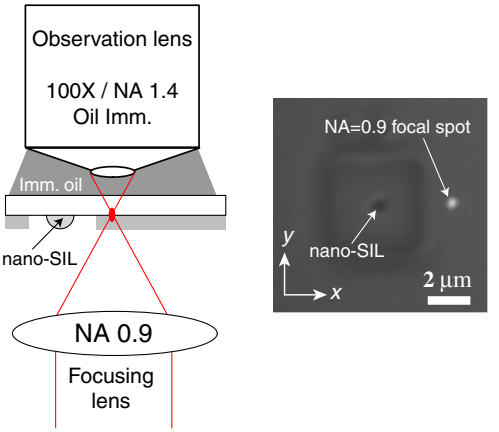

Fig. 6 (a) Schematic of the nonimmersion spot characterization and (b) corresponding CCD image (x – y plane) at the bottom of the SIL.

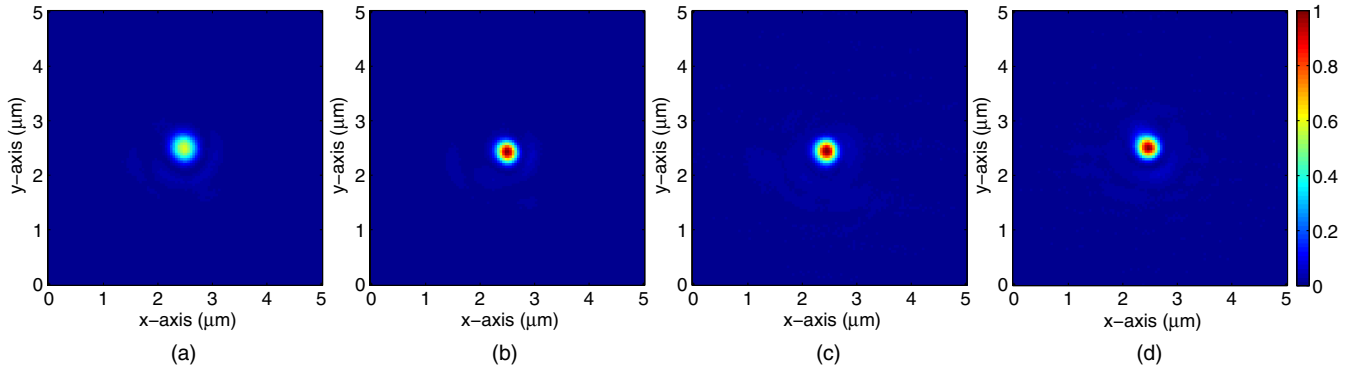

Fig. 7 (a) Reference spot, (b) the immersion spot of a circular nano-SIL [Fig. 4(a)], (c) the immersion spot of a square nano-SIL [Fig. 4(b)], and (d) the immersion spot of a triangular nano-SIL [Fig. 4(c)]. The intensities are normalized to the peak intensity of the immersion spots.

spot, which is shown in Fig. 7(a), shows the full width at half maximum spot size of approximately 400 nm when it is focused through the 250-nm-thick planar polymer layer.

Next, the reference focal spot is moved onto the nano-SILs, and the resulting immersed focal spots measured on the bottom of each SIL are shown in Fig. 7(b)–7(d). Compared with the reference spot in Fig. 7(a), the immersed spots show a higher peak intensity and smaller FWHM spot size due to the tighter confinement. The FWHM spot sizes are measured to be 302 nm, 321 nm, and 317 nm for the SILs shown in Fig. 4(a)–4(c), respectively. Although there are small differences in the spot size reduction ratio, the SILs exhibit an overall spot size reduction of approximately 1.3. Nonspherical nano-SILs show a comparable optical performance with that of the spherical SIL.

4 Conclusions

We have experimentally realized nanometer-scale SILs of different shapes in order to investigate the influence of the shape on the optical performance of the SIL. For reference, the ideal structure, i.e., a cylinder, was designed on the same chip with square and triangular pillars. Over-reflow leads to complete melting of the PMMA pillars, and ultimately the pillars of different shapes are converted to spherical SILs with a reduced height. We found the optimal reflow conditions to achieve the desired SIL height and to maintain the original shape of the pillar base. Using the HRIM, we measured the 3-D intensity distributions of immersed spots from the fabricated nano-SILs to show the reduction of the FWHM spot size. The overall reduction ratio for the FWHM spot size was found to be approximately 1.3, which is consistent with our previous findings.[13] The nonspherical SILs exhibit a comparable spot-size reduction to the spherical SIL. In this way, we experimentally verified the insensitivity to subtle variation of the base shape of the nano-SIL. We assume that when the SIL size falls in the wavelength scale or smaller, aberrations are negligible due to the short optical path length. This insensitivity to minor variations in shape implies a large tolerance in nano-SIL fabrication. Such nano-SILs find practical applications of near-field focusing and magnification combined with a conventional microscope.[11] The advantage of our technique is that we can precisely locate such nano-SILs on the target using e-beam lithography or vortex beam lithography.[22]

Acknowledgments

The research leading to these results has received funding from the European Space Agency (ESA), the Swiss National Science Foundation (SNSF), and the U.S. National Science Foundation (NSF).

References

1. R. Hooke, *Lectures and Collections; Microscopium*, Royal Society, London (1678).
2. D. Brocksch, "[Innovation] The Magazine form Carl Zeiss," Vol. 15, p. 8 (2005).
3. E. Abbe, "On new methods for improving spherical correction applied to the construction of wide-angled object-glasses," *J. Roy. Microsc. Soc.* **2**(7), 812–824 (1879).
4. E. Abbe, "On the estimation of aperture in the microscope," *J. Roy. Microsc. Soc.* **1**(3), 388–423 (1881).
5. S. M. Mansfield and G. S. Kino, "Solid immersion microscope," *Appl. Phys. Lett.* **57**(24), 2615–2616 (1990).
6. R. Brunner et al., "Diffraction-based solid immersion lens," *J. Opt. Soc. Am. A* **21**(7), 1186–1191 (2004).
7. D. A. Fletcher et al., "Microfabricated silicon solid immersion lens," *JMEMS*, **10**(3), 450–459 (2001).
8. M. Lang et al., "Investigation of micro solid immersion lens mounting systems," *Jpn. J. Appl. Phys.* **46**(6B), 3737–3740 (2007).
9. T. Kishia, S. Shibata, and T. Yano, "Fabrication of high-refractive-index glass micron-sized solid immersion lenses by a surface-tension mold technique," *J. Non-Cryst. Sol.* **354**(2–9), 558–563 (2008).
10. M. Brun, M. Richard, and S. Nicoletti, "Integrated micro solid immersion lens for near field optical data storage," in *Int. Symp. on opt. mem. (ISOM09)* (2009).
11. J. Y. Lee et al., "Near-field focusing and magnification through self-assembled nanoscale spherical lenses," *Nature* **460**, 498–501 (2009).
12. D. R. Mason, M. V. Jouravlev, and K. S. Kim, "Enhanced resolution beyond the Abbe diffraction limit with wavelength-scale solid immersion lenses," *Opt. Lett.* **35**(12), 2007–2009 (2010).
13. M.-S. Kim et al., "Subwavelength-size solid immersion lens," *Opt. Lett.* **36**(19), 3930–3932 (2011).
14. Ph. Nussbaum et al., "Design, fabrication and testing of microlens arrays for sensors and microsystems," *Pure Appl. Opt.* **6**(6), 617–636 (1997).
15. H. Ottevaere et al., "Comparing glass and plastic refractive microlenses fabricated with different technologies," *J. Opt. A: Pure Appl. Opt.* **8**(7), S407–S429 (2006).
16. Y. Xia and G. M. Whitesides, "Soft lithography," *Annu. Rev. Mater. Sci.* **28**(1), 153–184 (1998).
17. A. Schleunitz and H. Schift, "Fabrication of 3D nanoimprint stamps with continuous reliefs using dose-modulated electron beam lithography and thermal reflow," *J. Micromech. Microeng.* **20**(9), 095002 (2010).
18. H.-M. Lee et al., "New nanometer T-gate fabricated by thermally reflowed resist technique," *Jpn. J. Appl. Phys.* **41**, 1508–1510 (2002).
19. T. Grossmann et al., "High-Q conical polymeric microcavities," *Appl. Phys. Lett.* **96**(1), 013303 (2010).
20. M.-S. Kim, T. Scharf, and H. P. Herzig, "Small size microlenes characterization by multiwavelength high resolution interference microscopy," *Opt. Express* **18**(14), 14319–14329 (2010).
21. M.-S. Kim et al., "Engineering photonic nanojets," *Opt. Express* **19**(11), 10206–10220 (2011).

22. M.-S. Kim et al., "Low-NA focused vortex beam lithography for below 100-nm feature size at 405 nm illumination," in *Proc. SPIE* **8613**, 86131A (2013).

Myun-Sik Kim received his MS degree in mechatronics from the Gwangju Institute of Science and Technology (GIST), Korea, in 2004, and a PhD degree in photonics from the École Polytechnique Fédérale de Lausanne (EPFL), Switzerland, in 2011. Since August 2012, he has worked at SUSS MicroOptics SA (Hauterive, Switzerland) as a senior scientist in metrology and R&D. His research interests include physical optics, microoptics, and metrology. He is a member of OSA, OSK, EOS, SSOM, and SPIE.

Toralf Scharf received his MS degree from the University of Duisburg in surface physics, in 1993, and a PhD from the University of Halle, Germany. He has been a senior scientist at the Institute of Microtechnology in Neuchâtel before joining the École Polytechnique Fédérale de Lausanne (EPFL) in 2009. He focuses his research activities on interdisciplinary subjects bringing micro-system, material technology and optics together. He has a surface physics (MSc) and physical chemistry (PhD) background, with an extensive experience of over 15 years in optics. His activities are spanned from liquid crystal optics (book published with Wiley in 2006) to amorphous nanophotonics (book published in 2013). He is familiar with all necessary aspects of technology development and application and can communicate with different scientific communities.

David Nguyen received his BS degree in microengineering in 2012 from the École Polytechnique Fédérale de Lausanne (EPFL), where he is currently pursuing his MS degree in applied optics. His research interests include imaging optics and the nanotechnologies.

Ethan Keeler received his BS degree in electrical engineering from Montana State University in 2012. He is currently a research associate in the Department of Electrical and Computer Engineering at Montana State University in Bozeman, Montana. His current research involves the development and fabrication of nanostructures for interdisciplinary applications.

Skyler Rydberg received his BS degree in electrical engineering from Montana State University in 2013. He is currently an undergraduate research assistant at Montana State University in the Nano-Optics Group. In the summer of 2013, he will begin employment with GE Oil & Gas in the Edison Engineering Development Program.

Wataru Nakagawa received his BS degree in physics from Stanford University in 1996, and the MS and PhD degrees in electrical and computer engineering (applied physics) from the University of California, San Diego, in 1999 and 2002, respectively. He is currently an assistant professor in the Department of Electrical and Computer Engineering at Montana State University, in Bozeman, MT. His research interests include near-field optical effects in photonic structures and interdisciplinary applications of nanostructured optical devices. He is a senior member of the IEEE Photonics Society, and a member of OSA and SPIE.

Gaël Osowiecki received his bachelor's degree in micro- and nanotechnology from University of Neuchâtel (2009) and his master's degree in microtechnology from École Polytechnique Fédérale de Lausanne (EPFL) (2011). Since 2011 he has been a PhD student under the supervision of Prof. Hans Peter Herzig in the Optics & Photonics Technology Laboratory at EPFL. Technical: plasmonics, integrated waveguides, optical bio-sensors, fiber optics, EM simulations (CST MWS), optical design, MEMS, wafer-based micro-fabrication, interference lithography, photolithography, dry etching.

Reinhard Voelkel received his Diploma degree (1989) and the PhD degree (1994) in physics from the University of Erlangen, Germany, working with Prof. Adolf W. Lohmann and Prof. Johannes Schwider, respectively. He worked as post-doc/scientist at Institute of MicroTechnology in Neuchatel, Switzerland, working with Prof. Rene Dandliker and Prof. Hans Peter Herzig (1994–1999). He has been the cofounder and CEO of SUSS MicroOptics SA, Hauterive, Switzerland, since then. He has more than 25 years of experience in Optics, Micro-Optics, Optical Communication, Imaging Systems, Microtechnology and Semiconductor Manufacturing Technology.

Hans Peter Herzig received his Diploma degree in physics from the Swiss Federal Institute of Technology, Zurich, Switzerland, in 1978, and the Ph.D. degree in optics from the University of Neuchâtel, in 1987. From 1978 to 1982, he was a scientist in the Department of Optics Development of Kern, Aarau, Switzerland, working on lens design and optical testing. In 1983, he was a graduate research assistant with the Applied Optics Group, Institute of Microtechnology, University of Neuchâtel, Switzerland, working in the field of holographic optical elements. From 1989 to 2001, he was the head of the Micro-Optics Research Group. From 2002 to 2008, he was a full professor and the director of the Applied Optics Laboratory, University of Neuchâtel. He joined the faculty with the École Polytechnique Fédérale de Lausanne (EPFL), Switzerland, in 2009. Currently, he is a professor with the EPFL. His research interests include refractive and diffractive micro-optics, nano-scale optics, and optical microsystems.